Malaya Journal of Matematik, Vol. 8, No. 4, 2233-2242, 2020

https://doi.org/10.26637/MJM0804/0155

Non-Darcian Benard Marangoni Convection in a superposed fluid-porous layer with temperature dependent heat source

R. Sumithra[1], R. K. Vanishree[2] and Deepa R. Acharya[1]*

Abstract

The investigation of Non-Darcian Benard Marangoni Convection (NDBMC) is carried out in a Superposed Fluid-Porous (SFP) layer, which consists of an incompressible, sparsely packed single component fluid saturated porous layer above which lies a layer of the same fluid, with temperature dependent heat sources in both the layers. The upper surface of the SFP layer is free with Marangoni effects depending on Temperature, where the lower surface of the SFP layer is rigid. The thermal Marangoni numbers are obtained in closed form for two sets of thermal boundaries set (i) Adiabatic-Adiabatic and set (ii) Adiabatic-Isothermal. Influence of temperature dependent heat source in terms of internal Rayleigh numbers, viscosity ratio, Darcy Number, thermal diffusivity ratio on NDBMC, is investigated in detail.

Keywords

Darcy-Brinkman model, Superposed Fluid-Porous layer, Marangoni Convection, Temperature dependent heat source.

AMS Subject Classification

76B07.

[1] *Department of UG, PG Studies & Research in Mathematics, Government Science College Autonomous, Bengaluru, Karnataka, India.*
[2] *Department of Mathematics, Maharani's Science College for Women, Maharani Cluster University, Bengaluru, Karnataka, India.*
***Corresponding author**: [1] deeparacharya24@gmail.com
Article History: Received **14** September **2020**; Accepted **13** December **2020**

Contents

1. Introduction

Marangoni convection which is the convection due to surface tension, has many applications in engineering and geophysical problems. It occurs around vapor bubbles during nucleation and the growth of vapor bubbles resulting from the variation in surface tension caused by temperature and/or concentration variations along the surface of the bubble. Experimental tests and numerical analysis of nucleate boiling have shown that heat transfer resulting from Marangoni flow can be significant under microgravity and may also be important in earth's gravity. Marangoni-induced flow is also important in crystal growth melts, in which the flow produces undesirable effects under microgravity in the same manner as buoyancy-induced natural convection. Welding is a fabrication process where the Marangoni effect has to be account for. When the base metal during welding reaches its melting point, a weld pool forms. Marangoni forces within these pools can affect the flow and temperature distribution and modify the molten pool extension. This can potentially result in stresses within the material as well as deformation. The growth of crystals by various methods, oil re-covery in petroleum industry and energy storage are some of other important applications of Marangoni convection.

Some literature on Marangoni convection / flow are by Tatiana Gambaryan-Roisman (2010) has developed a model describing Marangoni convection, interface dynamics and evaporation in liquid films on composite substrates or substrates

of functionally graded materials. Alexander and Alexander (2010) considered two cases flat non-deformable and deformable surface and performed linear stability analysis and showed that in both cases of the upper surface monotonic and oscillatory modes exist. They determined convection thresholds and critical Marangoni numbers for monotonic as well as for oscillatory mode. M. S. Al-Qurashi (2013) obtained numerical solution for thermal convection in two porous layers. Flow in the upper layer is governed by Brinkman's equations model and in the lower layer is governed by Darcy's model using Legendre polynomials. Gangadharaiah (2015) studied the effects of thermal anisotropy and mechanical anisotropy on the onset of Bernard-Marangoni convection in composite layers with anisotropic porous material. The upper fluid surface, free to atmosphere was considered to be deformable. The eigen value problem was solved using a regular perturbation technique with wave number as perturbation parameter.

There is some literature available on convective instability with heat sources in single fluid / porous layers / superposed layers. Thirlby (1970) conducted a numerical study of steady laminar convection in an infinite horizontal layer of fluid bounded by a rigid plate above at constant temperature and bounded below by a thermal insulator with uniformly distributed heat sources. Tveitereid and Palm (1976) studied a motion for finite Prandtl numbers and small supercritical Rayleigh numbers by using amplitude expansion in a fluid layer with uniformly distributed internal heat sources. Clever (1977) made a study of stationary two dimensional convection in an internally heated, infinite Prandtl number, horizontal fluid layer bounded by rigid plates of unequal temperatures. Riahi (1984) carried out the investigation of nonlinear convection in a horizontal with internal heat source. Pal (2011) investigated about the combined effects of non-uniform heat source/sink and thermal radiation on heat transfer of a laminar boundary layer flow of an incompressible viscous fluid over an unsteady stretching permeable surface by Runge-Kutta-Fehlberg method. Siddheshwar and Stephen Titus (2013) analytically carried out the Rayleigh Benard Convections with variable heat source/sink using Fourier series. Mahabaleshwar *et.al*(2017) found the qualitative effect of variable internal heat source and variable gravity on the onset of convection in a horizontal fluid saturated sparsely packed porous layer using single term Galerkin technique. Elyazid Flilihi *et.al* (2017) performed a semi-analytical investigation to analyze the thermal convection flow with a radiation flux and a variable internal heat generation along an inclined plate embedded in a saturated porous medium. The flow in the porous medium was modeled with the Darcy-Brinkman law taking into account the convective term, while the temperature field was obtained from the energy equation. The resulting coupled differential equations were then solved numerically by a computational program based on the fifth order Runge-Kutta scheme with shooting iteration technique. Sumithra *et.al* (2020) investigated single component Marangoni convection in composite layer, comprising of an incompressible single component fluid saturated porous layer over which lies a layer of same fluid with constant heat sources in both the layers. This composite layer was subjected to linear, parabolic and inverted parabolic temperature profiles. A closed form solution was obtained for the thermal Marangoni numbers, which was an expression of various parameters. Here in this paper, an attempt is made to understand the effect of temperature dependent heat sources/sinks on NDBMC in a SFP layer. This SFP layer is bounded below and above by rigid and free boundaries with surface tension effects depending on temperature at the free boundary. The eigen value, the Thermal Marangoni Number (TMN) which the criterion for the onset of Marangoni convection is obtained for two cases of temperature boundary combinations, set (i) Adiabatic – Adiabatic and set (ii) Adiabatic – Isothermal.

2. Mathematical formulation

Consider a superposed fluid-porous (SFP) layer system consisting of a horizontal single component fluid saturated isotropic sparsely packed porous layer of thickness d_m and above this lies a layer of same fluid of thickness d, both the layers are with heat sources/sinks Q and Q_m depending on Temperature, respectively. The lower surface of the porous is rigid and the upper surface is free with Marangoni effects depending on temperature. Choose a Cartesian coordinate system where origin is taken to be at the interface between porous and fluid layer and z-axis is vertically upward.The governing equations for fluid layer are

$$\nabla.\vec{q} = 0 \tag{2.1}$$

$$\rho_0 \,[\frac{\partial \vec{q}}{\partial t} + (\vec{q}.\nabla)\vec{q}] = -\nabla P + \mu\nabla^2\vec{q} \tag{2.2}$$

$$\frac{\partial T}{\partial t} + (\vec{q}.\nabla)T = \kappa\nabla^2 T + Q(T - T_0) \tag{2.3}$$

and the same for porous layer

$$\nabla_m.\vec{q_m} = 0 \tag{2.4}$$

$$\frac{\rho_0}{\phi}\,[\frac{\partial \vec{q_m}}{\partial t_m}] = -\nabla_m P_m - \frac{\mu}{K}\vec{q_m} + \mu_m\nabla_m^2\vec{q_m} \tag{2.5}$$

$$A\frac{\partial T_m}{\partial t_m} + (\vec{q_m}.\nabla m)T_m = \kappa_m\nabla_m^2 T_m + Q_m(T_m - T_0) \tag{2.6}$$

Where, $\vec{q}$ is velocity vector, ρ_0 is fluid density, t is time, μ is fluid viscosity, P is Pressure, T is Temperature, κ is thermal diffusivity of the fluid, K is permeability of the porous medium, Q is heat source/sink for fluid layer, ϕ is porosity, A = $\frac{(\rho_0 C_p)_m}{(\rho_0 C_p)_f}$ ratio of heat capacities , C_p is Specific heat and the quantities with subscript 'm' denote the same in the porous layer and 'f' denotes the fluid layer.

The basic state of fluid and porous layer is quiescent, have the following solutions.

$$\vec{q} = \vec{q_b} = 0,\ P = P_b(z),\ T = T_b(z) \tag{2.7}$$

$$\vec{q_m} = \vec{q_{mb}} = 0,\ P_m = P_{mb}(z_m),\ T_m = T_{mb}(z_m) \tag{2.8}$$

The Temperature distributions $T_b(z)$ & $T_{mb}(z_m)$ are found to be

$$T_b(z) = \frac{(T_u - T_0)Sin(\sqrt{\frac{Q}{\kappa}}z)}{Sin(\sqrt{\frac{Q}{\kappa}}d)} + T_0,\ 0 \le z \le d \tag{2.9}$$

$$T_{mb}(z_m) = \frac{(T_0 - T_L)Sin(\sqrt{\frac{Q_m}{\kappa_m}}z_m)}{Sin(\sqrt{\frac{Q_m}{\kappa_m}}d_m)} + T_0,\ -d_m \le z_m \le 0 \tag{2.10}$$

Where,

$$T_0 = \frac{\sqrt{Q\ \kappa}\ T_u Sin(\sqrt{\frac{Q_m}{\kappa_m}}d_m) + \sqrt{Q_m\ \kappa_m}\ T_L Sin(\sqrt{\frac{Q}{\kappa}}d)}{\sqrt{Q_m\ \kappa_m}Sin(\sqrt{\frac{Q}{\kappa}}d) + \sqrt{Q\ \kappa}Sin(\sqrt{\frac{Q_m}{\kappa_m}}d_m)}$$

is the interface temperature and subscript 'b' denote the basic state.

We super impose infinitesimal disturbances on the basic state for fluid and porous layer respectively

$$\vec{q} = \vec{q_b} + \vec{q'},\ P = P_b(z) + P',\ T = T_b(z) + \theta \tag{2.11}$$

$$\vec{q_m} = \vec{q_{mb}} + \vec{q'_m},\ P_m = P_{mb}(z_m) + P'_m,\ T_m = T_{mb}(z_m) + \theta_m \tag{2.12}$$

Where, the prime indicates the perturbation quantities. The quantities with the subscript 'b' represent the quantities in basic state.

Introducing (2.11) and (2.12) in (2.1)-(2.3) and (2.4)-(2.6) respectively, operating curl twice to eliminate the pressure term from equations (2.2) and (2.5), then all the resulting equations then non-dimensionalised using appropriate scale factors according to Vanishree*et.al*(2020) and Sumithra *et.al*(2020).

The dimensionless equations are then subjected to normal mode analysis as follows:

$$\begin{bmatrix} W \\ \theta \end{bmatrix} = \begin{bmatrix} W(z) \\ \theta(z) \end{bmatrix} f(x,y)e^{nt} \tag{2.13}$$

$$\begin{bmatrix} W_m \\ \theta_m \end{bmatrix} = \begin{bmatrix} W_m(z_m) \\ \theta_m(z_m) \end{bmatrix} f_m(x_m, y_m)e^{n_m t_m} \tag{2.14}$$

With $\nabla_2^2 f + a^2 f = 0$ and $\nabla_{2m}^2 f_m + a_m^2 f_m = 0$, where a & a_m are wave numbers, n & n_m are the frequencies, W & W_m are the dimensionless vertical velocities in fluid and porous layer respectively & obtain the following equations.

In $0 \le z \le 1$

$$(D^2 - a^2 + \frac{n}{P_r})(D^2 - a^2)W = 0 \tag{2.15}$$

$$[(D^2 - a^2 + n + R_I)\theta + \frac{W\sqrt{R_I}Cos\sqrt{R_I}z}{Sin\sqrt{R_I}}] = 0 \tag{2.16}$$

In $-1 \le z_m \le 0$

$$(D_m^2 - a_m^2)\hat{\mu}Da + \frac{n_m Da}{P_{rm}} - 1](D_m^2 - a_m^2)W_m = 0 \tag{2.17}$$

$$[(D_m^2 - a_m^2 + n_m A + R_{Im})\theta_m + W_m\frac{\sqrt{R_{Im}}Cos\sqrt{R_{Im}}z_m}{Sin\sqrt{R_{Im}}}] = 0 \tag{2.18}$$

Where

$P_r = \frac{\mu}{\rho_0 \kappa}$ *is the Prandtl number*

$R_I = \frac{Q}{\kappa}d^2$ *is the internal Rayleigh number in fluid layer*

$\hat{\mu} = \frac{\mu_m}{\mu}$ *is the viscosity ratio*

$Da = \frac{K}{d_m^2}$ *is the Darcy number*

$P_{rm} = \frac{\mu\phi}{\rho_0 \kappa_m}$ *is the Prandtl number in porous layer*

$R_{Im} = \frac{Q_m}{\kappa_m}d_m^2$ *is the internal Rayleigh number in porous layer.*

Assume that the present problem satisfies the principle of exchange instability, so putting $n = n_m = 0$, the ordinary differential equations in $0 \le z \le 1$ & $-1 \le z_m \le 0$ respectively are

$$(D^2-a^2)^2W=0 \tag{2.19}$$

$$(D^2-a^2+R_I)\theta+\frac{W\sqrt{R_I}Cos\sqrt{R_I}z}{Sin\sqrt{R_I}}=0 \tag{2.20}$$

$$[(D_m^2-a_m^2)\hat{\mu}Da-1](D_m^2-a_m^2)W_m=0 \tag{2.21}$$

$$[(D_m^2-a_m^2+R_{Im})\theta_m+W_m\frac{\sqrt{R_{Im}}Cos\sqrt{R_{Im}}z_m}{Sin\sqrt{R_{Im}}}]=0 \tag{2.22}$$

Since the equations (2.19), (2.20), (2.21) and (2.22) are ODE's, to solve these equations, eight velocity boundary conditions and four temperature boundary conditions are needed.

3. Boundary Conditions

The suitable velocity and temperature Boundary conditions also non-dimensionalized and subjected to normal mode analysis and they are

Velocity boundary Conditions:

$$W(1)=0; W_m(-1)=0; W(0)=\frac{\zeta}{\varepsilon_T}W_m(0);$$

$$DW(0)=\frac{\zeta^2}{\varepsilon_T}D_mW_m(0);$$

$$D^2W(0)+a^2W(0)=\hat{\mu}\frac{\zeta^3}{\varepsilon_T}[D_m^2W_m(0)+a_m^2W_m(0)];$$

$$D_mW_m(-1)=0;$$

$$D^3W(0)-3a^2DW(0)=\frac{-\zeta^2}{Da\varepsilon_T}D_mW_m(0)+$$

$$\frac{\zeta^4}{\varepsilon_T}[D_m^3W_m(0)-3a_m^2D_mW_m(0)];$$

$$D^2W(1)+a^2M\theta(1)=0 \tag{3.1}$$

Temperature boundary Conditions:

Set (i) A-A, Adiabatic-Adiabatic temperature boundary conditions:

$$D\theta(1)=0; \qquad \theta(0)=\theta_m(0)\frac{\varepsilon_T}{\zeta};$$

$$D\theta(0)=D_m\theta_m(0); \qquad D_m\theta_m(-1)=0 \tag{3.2}$$

Set (ii) A-I, Adiabatic-Isothermal temperature boundary conditions:

$$D\theta(1)=0; \qquad \theta(0)=\theta_m(0)\frac{\varepsilon_T}{\zeta};$$

$$D\theta(0)=D_m\theta_m(0); \qquad \theta_m(-1)=0 \tag{3.3}$$

Where,

$$\zeta=\frac{d}{d_m} \text{ is the depth ratio}$$

$$\varepsilon_T=\frac{\kappa}{\kappa_m} \text{ is the thermal diffusivity ratio}$$

$$M=\frac{-(T_0-T_u)d}{\mu K}\frac{\partial\sigma}{\partial T} \text{ is the thermal Marangoni number}$$

Where, σ is the surface tension and T is the temperature.

4. Method of solution

Solution for W and W_m are obtained by solving the equations (2.19) and (2.21) by using the boundary conditions (3.1)

$$W(z)=A_1[Coshaz+A_2Sinhaz+A_3zCoshaz+A_4zSinhaz] \tag{4.1}$$

$$W_m(z_m)=A_1[A_{m1}Cosha_mz_m+A_{m2}Sinha_mz_m+A_{m3}Cosh\delta z_m+A_{m4}Sinh\delta z_m] \tag{4.2}$$

Where $A_2, A_3, A_4, A_{m1}, A_{m2}, A_{m3}, A_{m4}$ are constants determined by solving the boundary conditions (2.23) and they are as follows:

$$A_2=\frac{B_9A_{m2}+B_{10}A_{m4}}{B_8}; \quad A_3=\frac{a_mA_{m2}+\delta A_{m4}-aB_3A_2}{B_3}$$

$$A_4=\frac{B_6A_{m1}+B_7A_{m3}-aB_5}{B_5}; \quad A_{m1}=B_2-A_{m3};$$

$$A_{m2}=\frac{B_{11}A_{m1}+B_{13}A_{m3}-B_{14}A_{m4}}{B_{12}};$$

$$A_{m3}=\frac{-\Omega_{15}-\Omega_{14}A_{m4}}{\Omega_{13}}$$

$$A_{m4}=\frac{\Omega_{13}\Omega_{18}-\Omega_{15}\Omega_{16}}{\Omega_{16}\Omega_{14}-\Omega_{13}\Omega_{17}};$$

Where

$$\Omega_1=B_3B_5a-B_1B_3B_5; \quad \Omega_2=B_3B_5-B_1B_3B_5a;$$

$$\Omega_3=B_8\Omega_1-B_2B_3B_6B_8; \Omega_4=B_3B_7B_8-B_3B_6B_8;$$

$$\Omega_5=B_1B_5B_8a_m+\Omega_2B_9; \Omega_6=B_1B_5B_8\delta+\Omega_2B_{10};$$

$\Omega_7 = B_{11}B_2$; $\Omega_8 = B_{13} - B_{11}$; $\Omega_9 = -a_m B_{12}B_2$;

$\Omega_{10} = a_m B_{12} - \delta B_{14}$; $\Omega_{11} = a_m B_{11}$; $\Omega_{12} = \delta B_{13}$;

$\Omega_{13} = B_{12}\Omega_4 + \Omega_5\Omega_8$; $\Omega_{14} = B_{12}\Omega_6 - B_{14}\Omega_5$;

$\Omega_{15} = \Omega_5\Omega_7 - \Omega_3 B_{12}$; $\Omega_{16} = \Omega_{11}\Omega_8 + B_{12}\Omega_{10}$;

$\Omega_{17} = B_{12}\Omega_{12} - \Omega_{11}B_{14}$; $\Omega_{18} = \Omega_{11}\Omega_7 + \Omega_9 B_{12}$;

$B_1 = \frac{Cosha}{Sinha}$; $B_2 = \frac{\varepsilon_T}{\zeta}$; $B_3 = \frac{\varepsilon_T}{\zeta^2}$; $B_4 = \frac{\hat{\mu}\zeta^3}{2a\varepsilon_T}$;

$B_5 = \frac{2a\varepsilon_T}{\hat{\mu}\zeta^3}$; $B_6 = 2a_m^2$; $B_7 = \delta^2 + a_m^2$; $B_8 = -2a^3$;

$B_9 = \frac{-\zeta^2 a_m}{Da\varepsilon_T} + \frac{\zeta^4 a_m^3}{\varepsilon_T} - 3a_m^3$;

$B_{10} = \frac{-\zeta^2\delta}{Da\varepsilon_T} + \frac{\zeta^4\delta^3}{\varepsilon_T} - 3a_m^3\delta$;

$B_{11} = Cosha_m$; $B_{12} = Sinha_m$;

$B_{13} = Cosh\delta$; $B_{14} = Sinh\delta$;

Thermal Marangoni number(TMN) for set (i) Adiabatic-Adiabatic (A-A) temperature boundary condition:

Solving (2.20) and (2.22) we obtain θ and θ_m using the temperature boundary conditions (3.2)

$\theta(z) = A_1[A_5 Coshbz + A_6 Sinhbz] + f(z)$

Where, $b = \sqrt{a^2 - R_I}$

$\theta_m(z_m) = A_1[A_{m5} Coshb_m z_m + A_{m6} Sinhb_m z_m] + f(z_m)$

Where, $b_m = \sqrt{a_m^2 - R_{Im}}$

The coefficients A_5, A_6, A_{m5}, A_{m6} are obtained by solving $\theta(z)$ and $\theta_m(z_m)$ using the A-A temperature boundary conditions as follows:

$f(z) = S[I_1 + I_2 + I_3 + I_4]$

$f_m(z_m) = S_m[I_{m1} + I_{m2} + I_{m3} + I_{m4}]$

$S = \frac{-\sqrt{R_I}A_1}{Sin\sqrt{R_I}}$; $S_m = \frac{-\sqrt{R_{Im}}A_1}{Sin\sqrt{R_{Im}}}$

$I_1 = \frac{1}{2a\sqrt{R_I}} Sinhaz Sin\sqrt{R_I}z$; $I_2 = \frac{A_2}{2a\sqrt{R_I}} Sin\sqrt{R_I}z Coshaz$;

$I_3 = \frac{A_3}{2a\sqrt{R_I}}[zSin\sqrt{R_I}z Sinhaz - \frac{Sin\sqrt{R_I}z}{a} Coshaz +$

$\frac{Cos\sqrt{R_I}z}{\sqrt{R_I}} Sinhaz]$;

$I_4 = \frac{A_4}{2a\sqrt{R_I}}[zSin\sqrt{R_I}z Coshaz - \frac{Sin\sqrt{R_I}z}{a} Sinhaz +$

$\frac{Cos\sqrt{R_I}z}{\sqrt{R_I}} Coshaz]$;

$I_{m1} = \frac{A_{m1}}{2a_m\sqrt{R_{Im}}} Sinha_m z_m Sin\sqrt{R_{Im}}z_m$;

$I_{m2} = \frac{A_{m2}}{2a_m\sqrt{R_{Im}}} Cosha_m z_m Sin\sqrt{R_{Im}}z_m$;

$I_{m3} = \frac{Am3}{c^2 + 4\delta^2 R_{Im}}[2\delta\sqrt{R_{Im}} Sin\sqrt{R_{Im}} z_m Sinh\delta z_m +$

$c\, Cos\sqrt{R_{Im}} z_m Cosh\delta z_m]$;

$I_{m4} = \frac{Am4}{c^2 + 4\delta^2 R_{Im}}[2\delta\sqrt{R_{Im}} Sin\sqrt{R_{Im}} z_m Cosh\delta z_m +$

$c\, Cos\sqrt{R_{Im}} z_m Sinh\delta z_m]$;

$A_5 = \frac{\varepsilon_T}{\zeta}[A_{m5} - P_3] + P_2$; $A_6 = \frac{1}{b}[A_{m6} b_m - P_5 + P_4]$;

$A_{m5} = \frac{P_7 Coshb_m - P_6 Coshb}{bSinhbCoshb_m \frac{\varepsilon_T}{\zeta} + b_m Sinhb_m Coshb}$;

$A_{m6} = \frac{P_6 + b_m Sinhb_m A_{m5}}{b_m Coshb_m}$;

$P_7 = P_1 + P_5 Coshb + (\frac{\varepsilon_T}{\zeta} P_3 - P_2) bSinhb - P_4 Coshb$;

$P_6 = \frac{\sqrt{R_{Im}}}{Sin\sqrt{R_{Im}}}\{\frac{A_{m1}}{2a_m\sqrt{R_{Im}}}(-\sqrt{R_{Im}} Sinha_m Cos\sqrt{R_{Im}} -$

$a_m Cosha_m Sin\sqrt{R_{Im}}) + \frac{A_{m2}}{2a_m\sqrt{R_{Im}}}(\sqrt{R_{Im}} Cosha_m$

$Cos\sqrt{R_{Im}} + a_m Sinha_m Sin\sqrt{R_{Im}}) + \frac{A_{m3}}{c^2 + 4\delta^2 R_{Im}}$

$(-2\delta^2\sqrt{R_{Im}} Sin\sqrt{R_{Im}} Cosh\delta - 2\delta R_{Im} Cos\sqrt{R_{Im}} Sinh\delta$

$- c\delta Cos\sqrt{R_{Im}} Sinh\delta + c\sqrt{R_{Im}} Sin\sqrt{R_{Im}} Cosh\delta)$

$+ \frac{A_{m4}}{c^2 + 4\delta^2 R_{Im}}(2\delta^2\sqrt{R_{Im}} Sin\sqrt{R_{Im}} Sinh\delta$

$+ 2\delta R_{Im} Cos\sqrt{R_{Im}} Cosh\delta$

$+ c\delta Cos\sqrt{R_{Im}} Cosh\delta - c\sqrt{R_{Im}} Sin\sqrt{R_{Im}} Sinh\delta)\}$;

$P_5 = \frac{\sqrt{R_{Im}}}{Sin\sqrt{R_{Im}}}\{\frac{A_{m2}}{2a_m} + \frac{A_{m4}}{c^2 + 4\delta^2 R_{Im}}[2\delta R_{Im} + c\delta]\}$;

$P_4 = \frac{1}{2aSin\sqrt{R_I}}[A_2\sqrt{R_I} + A_3(\frac{a}{\sqrt{R_I}} - \frac{\sqrt{R_I}}{a})]$;

$P_3 = \frac{c\sqrt{R_{Im}} A_{m3}}{(c^2 + 4\delta^2 R_{Im}) Sin\sqrt{R_{Im}}}$; $P_2 = \frac{A_4}{2a\sqrt{R_I} Sin\sqrt{R_I}}$;

$P_1 = \frac{1}{2aSin\sqrt{R_I}}[\sqrt{R_I} SinhaCos\sqrt{R_I} + aCoshaSin\sqrt{R_I} +$

$A_2\sqrt{R_I} CoshaCos\sqrt{R_I} + A_2 aSinhaSin\sqrt{R_I}$

$+A_3(\sqrt{R_I}SinhaCos\sqrt{R_I}+aCoshaSin\sqrt{R_I}$
$+CoshaCos\sqrt{R_I}(\frac{a}{\sqrt{R_I}}-\frac{\sqrt{R_I}}{a})-SinhaSin\sqrt{R_I})$
$+A_4(\sqrt{R_I}CoshaCos\sqrt{R_I}+aSinhaSin\sqrt{R_I}$
$+SinhaCos\sqrt{R_I}(\frac{a}{\sqrt{R_I}}-\frac{\sqrt{R_I}}{a})-CoshaSin\sqrt{R_I})];$

From the last velocity boundary conditions in (3.1), we have

$$M=\frac{-D^2W(1)}{a^2\theta(1)} \tag{4.3}$$

And using the same condition for set (i) Adiabatic-Adiabatic condition, the TMN is

$$M_{AA}=\frac{Q_1}{Q_2}$$

Where,

$Q_1=(a^2+A_3a^2+2A_4a)Cosha+(A_2a^2+A_4a^2+2A_3a)Sinha;$

$Q_2=A_5Coshb+A_6Sinhb-\frac{1}{2aSin\sqrt{R_I}}[SinhaSin\sqrt{R_I}+$
$A_2CoshaSin\sqrt{R_I}+A_3(SinhaSin\sqrt{R_I}-\frac{CoshaSin\sqrt{R_I}}{a}+$
$\frac{SinhaCos\sqrt{R_I}}{\sqrt{R_I}})+A_4(CoshaSin\sqrt{R_I}-\frac{SinhaSin\sqrt{R_I}}{a}+$
$\frac{CoshaCos\sqrt{R_I}}{\sqrt{R_I}})]$

Thermal Marangoni number for set (ii) Adiabatic-Isothermal (A-I) temperature boundary condition:

Solving (2.20) and (2.22) we obtain θ and θ_m using the temperature boundary conditions (3.3)

$\theta(z)=A_1[A_5Coshbz+A_6Sinhbz]+f(z)$

Where, $b=\sqrt{a^2-R_I}$

$\theta_m(z_m)=A_1[A_{m5}Coshb_mz_m+A_{m6}Sinhb_m(z_m)]+f(z_m)$

Where, $b_m=\sqrt{a_m^2-R_{Im}}$

The coefficients A_5,A_6,A_{m5},A_{m6} are obtained by solving $\theta(z)$ and $\theta_m(z_m)$ using the A-I temperature boundary conditions as follows:

$f(z)=S[I_1+I_2+I_3+I_4]$

$f(z_m)=S_m[I_{m1}+I_{m2}+I_{m3}+I_{m4}]$

$S=\frac{-\sqrt{R_I}A_1}{Sin\sqrt{R_I}}\quad ;S_m=\frac{-\sqrt{R_{Im}}A_1}{Sin\sqrt{R_{Im}}}$

$I_1=\frac{1}{2a\sqrt{R_I}}SinhazSin\sqrt{R_I}z\ ;\ I_2=\frac{A_2}{2a\sqrt{R_I}}Sin\sqrt{R_I}zCoshaz\ ;$
$I_3=\frac{A_3}{2a\sqrt{R_I}}[zSinhazSin\sqrt{R_I}z-\frac{Sin\sqrt{R_I}z}{a}Coshaz+$
$\frac{Cos\sqrt{R_I}z}{\sqrt{R_I}}Sinhaz];$
$I_4=\frac{A_4}{2a\sqrt{R_I}}[zCoshazSin\sqrt{R_I}z-\frac{Sin\sqrt{R_I}z}{a}Sinhaz+$
$\frac{Cos\sqrt{R_I}z}{\sqrt{R_I}}Coshaz];$
$A_5=\frac{\varepsilon_T}{\zeta}[A_{m5}-P_3]+P_2;\quad A_6=\frac{1}{b}[A_{m6}b_m-P_5+P_4];$
$A_{m5}=\frac{P_7Sinhb_m+P_6b_mCoshb}{bSinhbSinhb_m\frac{\varepsilon_T}{\zeta}+b_mCoshbCoshb_m};$
$A_{m6}=\frac{A_{m5}Coshb_m-P_6}{Sinhb_m};$
$P_7=P_1+P_5Coshb+(\frac{\varepsilon_T}{\zeta}P_3-P_2)bSinhb-P_4Coshb;$
$P_6=\frac{\sqrt{R_{Im}}}{Sin\sqrt{R_{Im}}}\{\frac{A_{m1}}{2a_m\sqrt{R_{Im}}}(Sinha_mSin\sqrt{R_{Im}})-$
$\frac{A_{m2}}{2a_m\sqrt{R_{Im}}}(Cosha_mSin\sqrt{R_{Im}})$
$+\frac{A_{m3}}{c^2+4\delta^2R_{Im}}(2\delta\sqrt{R_{Im}}Sinh\delta Sin\sqrt{R_{Im}}$
$+cCosh\delta Cos\sqrt{R_{Im}})+$
$\frac{A_{m4}}{c^2+4\delta^2R_{Im}}$
$(-2\delta\sqrt{R_{Im}}Cosh\delta Sin\sqrt{R_{Im}}-cSinh\delta Cos\sqrt{R_{Im}})\};$

$P_4=\frac{1}{2aSin\sqrt{R_I}}[A_2\sqrt{R_I}+A_3(\frac{a}{\sqrt{R_I}}-\frac{\sqrt{R_I}}{a})];$
$P_3=\frac{c\sqrt{R_{Im}}A_{m3}}{(c^2+4\delta^2R_{Im})Sin\sqrt{R_{Im}}}\ ;\ P_2=\frac{A_4}{2a\sqrt{R_I}Sin\sqrt{R_I}};$
$P_1=\frac{1}{2aSin\sqrt{R_I}}[\sqrt{R_I}SinhaCos\sqrt{R_I}+aCoshaSin\sqrt{R_I}+$
$A_2\sqrt{R_I}CoshaCos\sqrt{R_I}+A_2aSinhaSin\sqrt{R_I}+$
$A_3(\sqrt{R_I}SinhaCos\sqrt{R_I}+aCoshaSin\sqrt{R_I}+CoshaCos\sqrt{R_I}$
$(\frac{a}{\sqrt{R_I}}-\frac{\sqrt{R_I}}{a})-SinhaSin\sqrt{R_I})$
$+A_4(\sqrt{R_I}CoshaCos\sqrt{R_I}+aSinhaSin\sqrt{R_I}$
$+SinhaCos\sqrt{R_I}(\frac{a}{\sqrt{R_I}}-\frac{\sqrt{R_I}}{a})-CoshaSin\sqrt{R_I})];$

From the Boundary Conditions, we have

$$M=\frac{-D^2W(1)}{a^2\theta(1)} \tag{4.4}$$

And using the same condition for set (ii) Adiabatic-Isothermal condition, the TMN is

$$M_{AI} = \frac{Q_3}{Q_4}$$

Where

$$Q_3 = (a^2 + A_3a^2 + 2A_4a)Cosha + (A_2a^2 + A_4a^2 + 2A_3a)Sinha;$$

$$Q_4 = A_5Coshb + A_6Sinhb - \frac{1}{2aSin\sqrt{R_I}}[SinhaSin\sqrt{R_I} + A_2CoshaSin\sqrt{R_I} + A_3(SinhaSin\sqrt{R_I} - \frac{CoshaSin\sqrt{R_I}}{a} + \frac{SinhaCos\sqrt{R_I}}{\sqrt{R_I}}) + A_4(CoshaSin\sqrt{R_I} - \frac{SinhaSin\sqrt{R_I}}{a} + \frac{CoshaCos\sqrt{R_I}}{\sqrt{R_I}})]$$

5. Results and Discussions

The effect of Darcy-Brinkman Marangoni convection in a SFP system consisting of a fluid layer overlying a porous layer saturated by the same system in the presence of temperature dependent heat source is investigated theoretically. The eigen value problem is solved exactly and an analytical expression for the TMN, M as a function of various parameters of the system, is obtained for two types of temperature boundary conditions, viz (i) both the boundaries of the SFP layer are adiabatic A-A , (ii) lower rigid boundary is isothermal and upper free surface is adiabatic A-I. The effects of R_I, R_{Im} the internal Rayleigh numbers for the fluid and porous layers, the horizontal wave number 'a' , the thermal diffusivity ratio 'ε_T' and the Darcy number 'Da' on the TMN, M against the depth ratio ζ are displayed in the following figures (1)-(6).

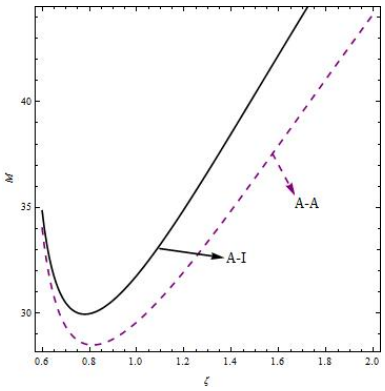

Figure 1. Comparison of thermal Marangoni number for A-A and A-I

The effect of different temperature boundary conditions (A-A and A-I) on TMNs as a function of depth ratio 'ζ' is shown in Fig (1). It is observed that in both the cases, TMNs, M_{AA} and M_{AI}, decreases initially with ζ and reaches minimum and then increases with further increase in ζ. It is also observed that $M_{AA} < M_{AI}$. The minimum values of M in the case of A-A boundaries occur at ζ=0.8 whereas for A-I boundaries, the minimum TMN occurs at ζ slightly less than 0.8. Beyond these values of ζ for the corresponding cases, M increases. When ζ is small, it implies that the system is dominated by porous layer. For the figures (2)-(6) the variation of TMN is shown for fixed values of a=1.1, Da=1.0, ε_T= 0.5, $\hat{\mu}$= 1.5, R_I= -0.5, R_{Im}= -0.5.

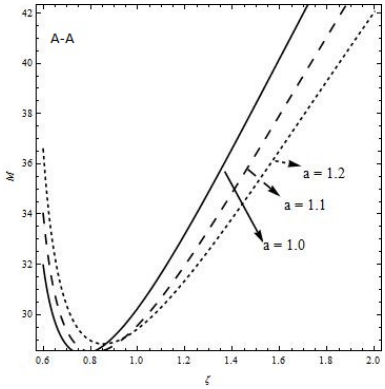

(a)

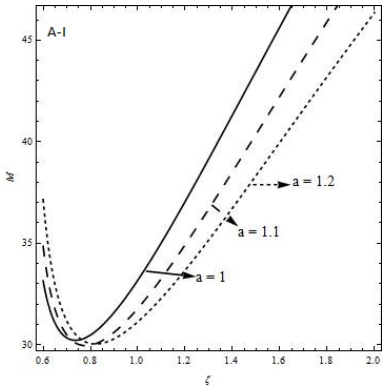

(b)

Figure2: Effects of wave number 'a'

Figures 2(a) and 2(b) are the plots of M_{AA} and M_{AI} versus the depth ratio ζ for linear temperature distribution for different wave numbers 'a'= 1.0, 1.1, 1.2, when the other parameters are fixed. From Fig. 2(a), it is clear that increasing cell size increase the TMN, M in the porous layer dominated SFP layer and the trend is reversed as the value of ζ increases. All the three curves for different values of 'a' coincide at a value of ζ between 0.8 and 1.0, after which M is seen decreasing for increasing 'a'. However, M increases with increase in ζ in this region of fluid dominant SFP layer and the reverse is happening in the porous layer dominant SFP layer. The difference in the values of TMNs for different wave numbers is small for ζ <1.0 compared to the difference in the values of TMNs for ζ >1.0. The results are qualitatively similar in the case of A-I as depicted in figure 2(b).

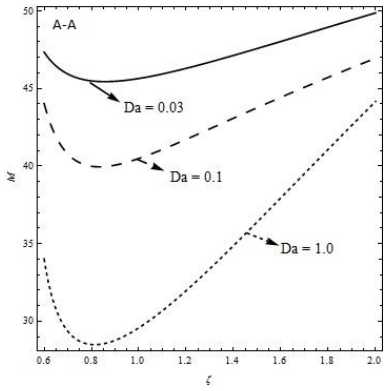

(a)

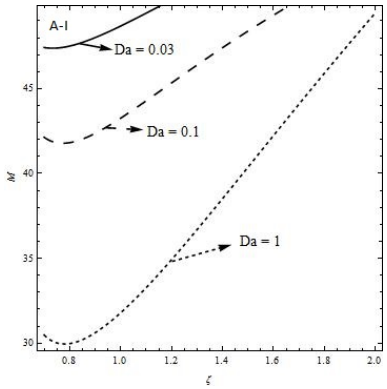

(b)

Figure3: Effects of Darcy number 'Da'

Figures 3(a) and 3(b) are the plots of M versus ζ for linear temperature distribution for different Darcy number 'Da' = 0.03, 0.1, 1.0. The effect of Da for a set of fixed values of other physical parameters a=1.1, R_{Im}=-0.5 ,ε_T=0.5 , R_I= -0.5, $\hat{\mu}$=1.5 in case of both A-A and A-I boundaries is to decrease M initially for small values of ζ (porous layer dominant SFP layer) and then increase. It can be seen that the effect of Da is to decrease the TMN, M in the case of both A-A and A-I boundaries.

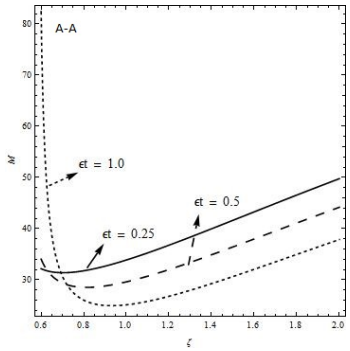

(a)

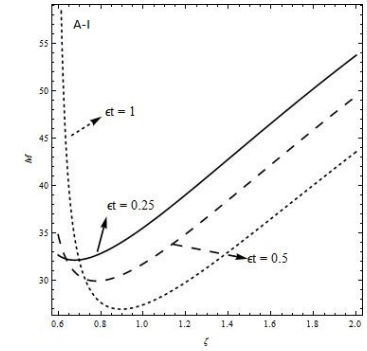

(b)

Figure4: Effects of Thermal diffusivity 'ε_T'

The effect of ε_T on TMN, M, as a function of ζ is shown in Figs. 4(a) and 4(b), respectively for fixed values of the remaining parameters. It is observed that TMN, M in both the cases (A-A and A-I boundaries), is maximum when the thermal diffusivity of fluid and porous medium are equal, for small values of depth ratio ζ. One can observe that,$\{M_{AA}(\zeta)\}_{(\varepsilon_T=1)} > \{M_{AI}(\zeta)\}_{(\varepsilon_T=1)}$ for porous layer dominant SFP layer. For smaller values of ζ, i.e., the porous layer dominant SFP layer increase in thermal diffusivity ratio ε_T increases TMN, and the trend reverses for larger values of ζ . This is because, decrease in temperature increases the surface tension.

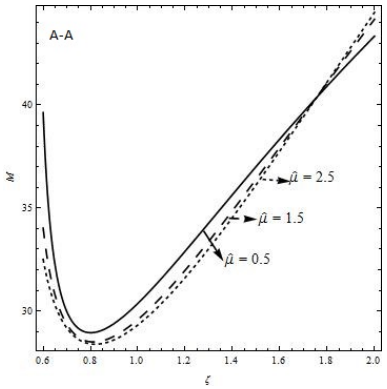

(a)

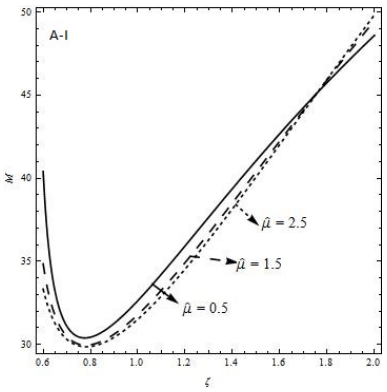

(b)

Figure5: Effects of Viscosity ratio 'μ'

Figures 5(a)and 5(b) depict the effect of viscosity ratio '$\hat{\mu}$' for a set of fixed parameters a=1.1, ε_T=0.5, Da= 1.0, R_I= -0.5,R_{Im}= - 0.5, on TMN M, as a function of ζ for both A-A and A-I boundaries. From these figures, it is clear that both $M_{AA}$and M_{AI} decrease initially attains minimum and increases with further increase in ζ.The effect of $\hat{\mu}$ is to decrease M. However, beyond the value of ζ =1.7 the effect of $\hat{\mu}$ is seen to increase M. This might be due to the fact that, this region is fluid layer dominant SFP layer and viscosity being the property of the fluid, will stabilize the system.

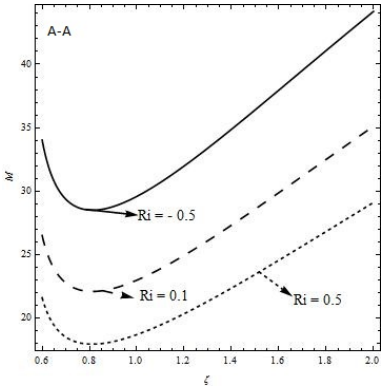

(a)

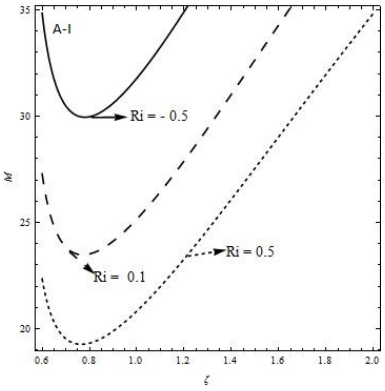

(b)

Figure6: Effects of Internal Rayleigh number 'R_I' for fluid layer

Figures 6(a) and 6(b) are the plots of TMN, M vs. ζ for different values of internal Rayleigh number for fluid layer, R_I. The positive and negative values of R_I indicate the strength of heat source and heat sink respectively. From these figures one can conclude that, in the case of both A-A and A-I boundaries, heat sink is more stabilizing than the source. This is once again due to the fact that, heat source adds to the temperature there by decreasing the surface tension and hence decrease in the TMN. The effect of ζ on M is similar to that found in the previous figures. We observe that M_{AI}, increases more rapidly than M_{AA} for a given value of ζ.

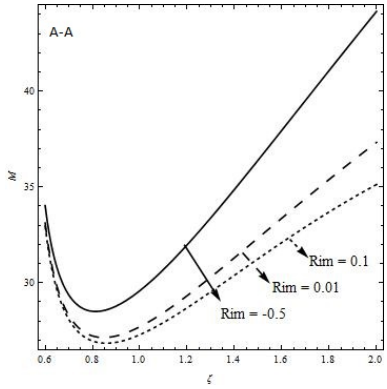

(a)

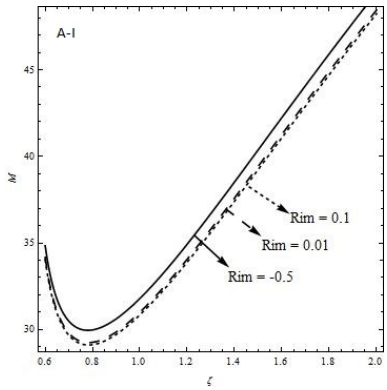

(b)

Figure7: Effects of Internal Rayleigh number 'R_{Im}' for porous layer

Figures 7(a) and 7(b) represent the changes in the TMN, M vs. ζ for different values of internal Rayleigh number in porous layer, R_{Im} when a=1.1, $\hat{\mu}$=1.5, ε_T= 0.5, Da=1.0, R_I= -0.5. In case of both A-A and A-I boundaries, we observe that M decreases initially attains minimum and then increases with increase in ζ. The effect of R_{Im}, (from sink to source) is to destabilize the system. This effect is similar to that of R_I. The effect of R_{Im} is more intensive for SFP layers with A-A thermal boundaries.

6. Conclusion

Darcy-Brinkman-Marangoni convection in a composite system with variable heat source is studied analytically and the results are discussed in the previous section. From these results following conclusions can be drawn:

1. $M_{AI}(\zeta) > M_{AA}(\zeta)$ for all the parameters except $\varepsilon_T = 1$, in figures 4a and 4b.

2. Heat source or sink can be effectively used to control convection.

3. Except for the case of Da, R_I and R_{Im}, the reversal of results is observed after a certain value of ζ for remaining parameters.

References

[1] Alexander B. Mikishev and Alexander A. Nepomnyashchy(2010), Long-Wavelength Marangoni Convection in a Liquid Layer with Insoluble Surfactant: Linear Theory, *Microgravity Science and Technology*, 22(2010), 415–423.

[2] Al-Qurashi M. S, A Study of Thermal Convection in Two Porous Layers Governed by Brinkman's Model in Upper Layer and Darcy's Model in Lower Layer, *World Academy of Science, Engineering and Technology International Journal of Physical and Mathematical Sciences,* 7(3)(2013).

[3] Clever, R. M., "Heat Transfer and Stability Properties of Convection Rolls in an Internally Heated Fluid Layer", *Z. Angew Math. Phys*, 28(1977), 585-597.

[4] A. Anguraj and P. Karthikeyan, Anti periodic boundary value problem for impulsive fractional integro differential equations, *Fract. Calc. Appl. Anal.,* 3(2010), 281-294.

[5] Elyazid Flilihia, Mohammed Sritia, Driss Achemlalb, Mohamed Elharouia, *Variable heat source and wall radiation effects on boundary layer convection from an inclined plate in Non-Darcian porous medium*, (2017). http://www.ThermalFluidsCentral.org.

[6] Ganesan Rajamohana,Narayanaswamy Ramesh, Perumal Kumar, *Mixed convection and radiation studies on thermally developing laminar flow in a horizontal square channel with variable side heated wall*, (2019). https://doi.org/10.1016/j.ijthermalsci.2019.03.002.

[7] Gangadharaiah.Y.H, Onset of Benard–Marangoni Convection in a Composite Layer with Anisotropic Porous Material, *Journal of Applied Fluid Mechanics*, 9(3)(2013), 1551-1558,

[8] Mahabaleshwara U.S, Basavaraja D, Shaowei Wang, Giulio Lorenzini, Enrico Lorenzini, Convection in a porous medium with variable internal heat source and variable gravity, *International Journal of Heat and Mass Transfer,* 111(2017), 651–656.

[9] Pal, D., combined effects of non-uniform heat source/sink and thermal radiation on heat transfer over an unsteady stretching permeable surface, *Commun. Nonlinear Sci. Numer. Simulat,* 16(2011), 1890-1904.

[10] N. S. Boris, A fixed point principle, *Functional Analysis and its Applications*, (1967), 151–153.

[11] Riahi, N., Nonlinear Convection in a Horizontal Layer with an Internal Heat Source, *J.Phys. Soc. Jpn*, 53(1984), 4169-4178.

[12] Siddheshwar, P. G., and Stephen Titus, P., Nonlinear Rayleigh–Bénard Convection with Variable Heat Source, *ASME. J. Heat Transfer,* 135(12)(2013), 122502.

[13] Sumithra R, Manjunatha N and Komala B, Effects of heat source/sink and non-uniform temperature gradients on non-darcian-benard-magneto-marangoni convection in an infinite horizontal composite layer, *Journal of Xidian University*, 14(5)(2020).

[14] Sumithra R, Nazhath Farhana ., Noor Ayesha S., and Malashri C.M, "The single component Marangoni Convection in a composite layer where both the lower and upper boundaries are isothermal" in the *proceedings of National conference titled Student & Faculty Research in Mathematical Sciences,* 2018.

[15] Sumithra R., Sowmyashree M., Mahalakshmi N. and Pallavi H.T, "*The single component Marangoni Convection in a composite layer where both the lower and upper boundaries are adiabatic*" in the proceedings of National conference titled Student & Faculty Research in Mathematical Sciences, 2018.

[16] Tatiana Gambaryan-Roisman, *Marangoni convection, evaporation and interface deformation in liquid films on heated substrates with non-uniform thermal conductivity,* (2010).

[17] Thirlby, R., Convection in an Internally Heated Layer, *J. Fluid Mech.*, 44(1970), 673-693.

[18] Tveitereid, M., and Palm, E., Convection Due to Internal Heat Sources, *J. Fluid Mech.*, 76(3)(1976), 481-499.

[19] Vanishree R K, Sumithra R and Manjunatha N, Effect on uniform and non uniform temperature gradients on Benard-Marangoni convection in a superposed fluid and porous layer in the presence of heat source, *GEDRAG & ORGANISATIE REVIEW*, 33(02)(2020).

[20] Zhang Yan, Zheng Liancun, Wang Xiaojing, Song Guhua, Analysis of Marangoni convection of non-Newtonian power law fluids with temperature distribution, *Thermal Science,* 15(1)(2011), 45-52.

★★★★★★★★★
ISSN(P):2319 – 3786
Malaya Journal of Matematik
ISSN(O):2321 – 5666
★★★★★★★★★